Open Access Articles

Graphene Biotransistor Interfaced with a Nitrifying Biofilm

Oregon State
UNIVERSITY

Graphene Biotransistor Interfaced with a Nitrifying Biofilm

Morgan A. Brown[1], Leila Barker[2], Lewis Semprini[2] and Ethan D. Minot[1]

[1]Department of Physics, Oregon State University

[2]School of Chemical, Biological and Environmental Engineering, Oregon State University

Abstract

Using a graphene field-effect transistor biosensor, we monitored the pH inside a living biofilm with fast temporal resolution (~ 1 s) over multi-hour time periods. The atomically-thin sensor is positioned between the biofilm and a supporting silicon oxide surface, providing non-invasive access to conditions at the base of the biofilm. We determine the transient changes in pH when the biofilm metabolizes substrate molecules and when it is exposed to biocide. The pH resolution is approximately 0.01 pH units when using 1-second time averaging. The sensor drift is approximately 0.01 pH units per hour. Our results demonstrate the potential of this technology to study biofilm metabolism and monitor biofilm health.

Introduction

Quantitative tools to monitor living biofilms are important in fields ranging from medicine to environmental monitoring. In applications, such as wastewater treatment, biofilm reactor systems are typically monitored using bulk fluid measurements.[1] This technique is powerful, because a range of traditional chemical assays are available and measurements are directly linked to process performance. However, it is well know that understanding the kinetics of growth and substrate utilization within a biofilm is essential for optimizing fixed-film processes.[2] Microsensors have been used to measure chemical gradients in biofilms including specific chemicals, such as dissolved oxygen, sulfide, nitrate, nitrite, and pH.[3,4] pH microelectrodes commonly used in biofilm studies have an H^+ selective membrane made of special glass. While they have a long lifetime, their spatial resolution is limited to about 20 μm and they are expensive.[4] Liquid ion-exchange (LIX) pH microsensors have a higher spatial resolution of ~ 5 μm, but have a short lifetime of only a few days.[4] Thus, there is interest to develop inexpensive long-lived sensors that have high spatial resolution.

Recent advances in bioelectronic sensors made from nanoscale materials offer exciting new ways to monitor biofilm activity. The goal of this study is to explore the suitability of field-effect transistor (FET) biosensors for monitoring the metabolic activity of a biofilm.

We use graphene, an atomically-thin sheet of sp^2-bonded carbon atoms, as the active material for our FET biosensor. The electrical resistance of graphene is sensitive to charged species adsorbed on the graphene surface.[5] Graphene is remarkably biocompatible, as shown by recent tests with *Escherichia coli*[6] and neural cells.[7] While graphene FET (GFET) biosensors are being

pursued by a number of research groups (reviewed in Ref [5] and [8]), efforts to interface GFETs with bacteria are just beginning. Previous authors have used chemically-functionalized graphene to capture bacteria on GFET sensors,[9,10,11] but there are no previous reports of naturally-formed biofilms interfaced with GFET sensors.

The biofilm used for this work is formed by ammonia oxidizing bacteria (AOB). AOB play a critical role in the global nitrogen cycle and in the removal of nitrogen during wastewater treatment.[12,13] Since AOB are slow growing, biofilm-based processes are particularly important. In the biofilm form, AOB exhibit higher nutrient removal rates and higher resistance to washout when compared to planktonic bacteria.[14] Techniques to monitor the health of AOB biofilms are desired, because AOB are considered to be some of the most sensitive microorganisms found in wastewater treatment plants.[15]

Methods

The GFET was fabricated using graphene grown via chemical vapor deposition.[16,17] Details of the fabrication process are described in Supporting Information. To limit the contact between liquid and electrical connections, the electrode traces were covered by 70 nm of SiO_2 and wires were sealed with silicone. Parasitic currents were 3 orders of magnitude smaller than the source drain current (I_{sd}). For all sensing experiments, the GFET was biased with a source-drain voltage V_{sd} = 25 mV. The electric potential of the liquid was controlled by an Ag/AgCl reference electrode attached to a voltage source, V_{liq} (see Fig. 1c).
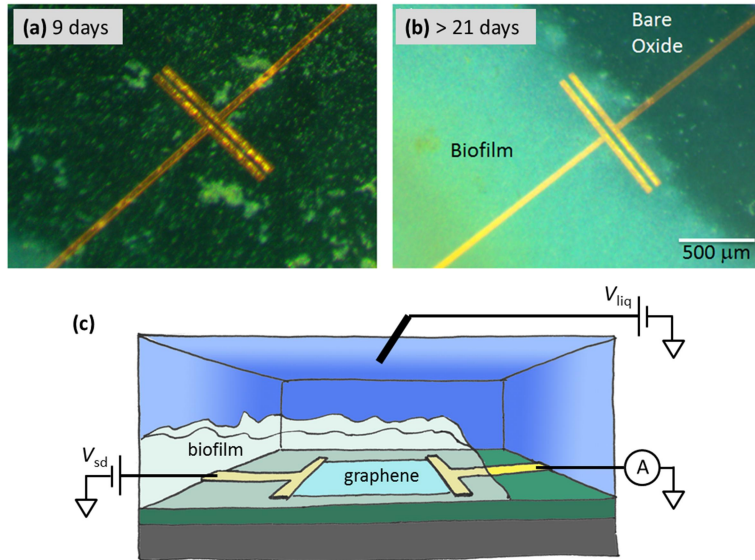
Figure 1. (a) Optical micrograph, 9 days growth, showing initial pillar formation. (b) Optical micrograph, > 21 days growth, showing the presence of a mature biofilm covering the GFET. The graphene sheet connecting the metal electrodes has an area of 40 μm x 1 mm. (c) Schematic diagram of the electrical measurement.
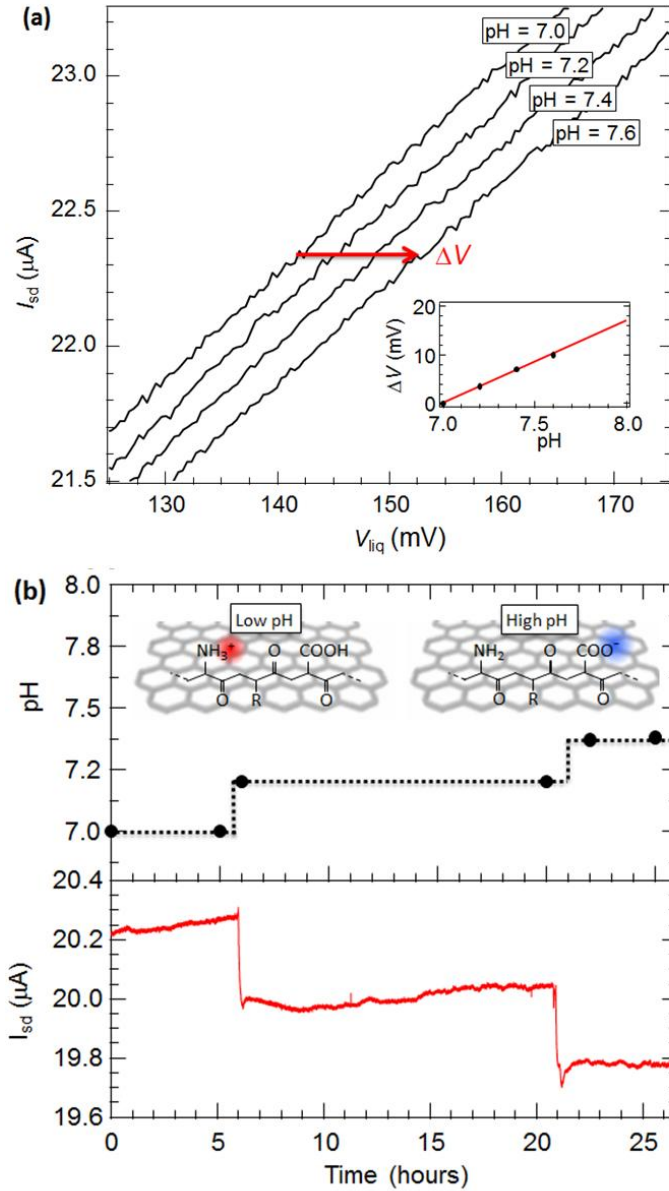
Figure 2. (a) Current through the bare graphene sensor, Isd, versus the electric potential of the liquid, Vliq, at different pH. The Isd-Vliq curve shifts rightward by □V when pH is increased. Similar curves were obtained after biofilm attachment (not shown). (b) After biofilm attachment, Isd(t) is monitored while changing the pH of the bulk liquid. Vliq = 150 mV. Biological

processes were shutdown during this test by using a nutrient-free buffer (6 mM HEPES). Insets illustrate changing surface charge associated with changing pH.

Prior to biofilm growth, we characterized the sensitivity of the bare GFET to pH (Fig. 2a). The device was operated with V_{liq} in the range $100 - 250$ mV where the slope $dI_{sd}/dV_{liq} = 39$ μA/V. Changing the pH by one unit was equivalent to a changing V_{liq} by $\Delta V = 17$ mV. Similar pH sensitivities have been observed by other authors and attributed to specific adsorption of hydroxyl and hydronium ions on the graphene surface.[18] Mailly-Giacchetti et al. verified that the linear relationship between ΔV and pH extends from pH 4 to above pH 8.[18] Therefore, for the pH conditions inside our AOB biofilms, the GFET can be operated at fixed V_{liq} to generate an I_{sd} signal that is linearly proportional to pH.

The AOB biofilm (*Nitrosomonas europaea*) was grown directly on the surface of the GFET device. The sensor was submersed in a bath of HEPES buffer (30 mM) with trace nutrients for growth.[19] The volume of liquid was maintained at approximately 60 mL in a standard petri dish. The GFET remained in this bath for the duration of the experiments. The *N. europaea* cells (ATCC strain 19718) used to inoculate the GFET surface were grown in batch, concentrated, and the cells and growth media, including biomolecules, were added to the petri dish.

The initial bacterial attachment phase lasted ~ 8 hours, during which bacteria, protein, and polysaccharides floating in solution gradually attached to the surface of the GFET. During this 8 hour period we observed changes in the I_{sd}-V_{liq} curve equivalent to $\Delta V = 60$ mV (Figure S5). Such changes in ΔV are consistent with charged molecules adsorbing on the graphene surface.[8]

After the initial bacterial attachment, the position of the $I_{sd}(V_{liq})$ curve became stable ($d\Delta V/dt \sim$ +/-0.2 mV/hour, corresponding to a baseline drift of 0.01 pH units per hour) and the device exhibited greater pH sensitivity (1.4 µA/pH) (Fig. 2b). The augmented pH sensitivity of the GFET sensor is likely due to new ionizable groups on the graphene surface,[20,21,8] as illustrated in Fig 2b inset. The pH-dependent charge state of moieties such as COOH and NH_2 modifies the number of charge carriers in the graphene, causing changes in I_{sd}.

Results and Discussion

Optical micrographs were taken to determine biofilm development on the GFET. These images show pillar formation, followed by the development of mature biofilms in a timeframe of approximately 2.5 weeks (see Fig. 1a and b). Similar timescales for *N. europaea* biofilm development were observed by Lauchnor et al.[19] To confirm that the biofilm was indeed an AOB, rather than an unwanted bacterium, we used traditional methods to monitor the nitrite and pH levels of the bulk fluid over four days (Figure S6). We observed a continuous increase in nitrite levels and decrease in pH, consistent with the activity of an AOB and consistent with *N. europaea* batch tests at a similar buffer capacity.[22]

While establishing the biofilm, the medium was exchanged regularly to replace nutrients and buffer and to remove bacteria suspended in solution. After a mature biofilm was established, roughly 3 weeks, the GFET was used to monitor pH at the base of the biofilm with high temporal resolution. We first studied the response of the system to ammonia (NH_3). *N. europaea* is known to convert NH_3 to NH_2OH and then NO_2^- in a two-step process. The enzyme ammonia mono-oxygenase (AMO) catalyzes the first step, and hydroxylamine oxidoreductase (HAO) catalyzes the second step.

$$NH_3 + 3/2\ O_2 \xrightarrow{\text{(AMO+HAO)}} NO_2^- + H^+ + H_2O \qquad (1)$$
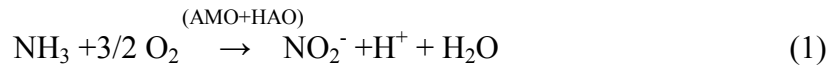
The balanced reaction for NH_3 oxidation to NO_2^-, (equation 1) shows that one H^+ is released per NH_3 molecule oxidized. The net result is a more acidic environment; therefore, the consumption of NH_3 by *N. europaea* is well suited to monitoring via the pH sensitive GFET.

Prior to making a GFET measurement, the media was exchanged for one with a lower buffer capacity (6 mM HEPES).[22] Low buffer capacity optimized pH sensitivity and the fresh media ensured that subsequent nitrification activity was associated with the biofilm rather than suspended bacteria. Substrate utilization was initiated by introducing $(NH_4)_2SO_4$ into the 60 mL volume of buffer solution to produce an NH_4^+ concentration of ~ 1 mM. The $(NH_4)_2SO_4$ aliquot was added slowly to the bulk fluid at the side of the petri dish, taking care to avoid mechanical disturbance to the biofilm which was positioned at the center of the petri dish. At pH 7.5, only a fraction of NH_4^+ ions are present in the biologically-available NH_3 form (~ 16 μM). This concentration is approximately 25 % the saturation coefficient (K_s) for NH_3 for *N. europaea*.[23]

The green trace in Figure 3 shows the typical sensor response. Before introducing NH_3, the sensor was calibrated by measuring the pH of the bulk fluid (black cross at $t = 16$ min). Previous work by Lauchnor[24] using a pH microelectrode, found that in the absence of NH_3 oxidation the pH in a biofilm of *N. Europaea* was the same as the bulk solution. After introducing NH_3, the sensor reports a gradual decrease in pH, followed by a slight rise to a stable value. At $t = 80$ minutes, the pH measured by the GFET differs slightly from the bulk pH, however, the difference is within the baseline drift expected for an 80 minute recording. Nitrite levels in the bulk fluid were also checked at $t = 18$ and 80 min. Nitrite concentration increased from 3.04 to 3.46 mM. Of the 1.0 mM NH_4^+ added, 0.4 mM was converted to NO_2^-. It should be noted that as

NH$_3$ is consumed, the equilibrium NH$_4^+$ ⇌ NH$_3$ + H$^+$ is maintained and NH$_4^+$ is converted to NH$_3$.
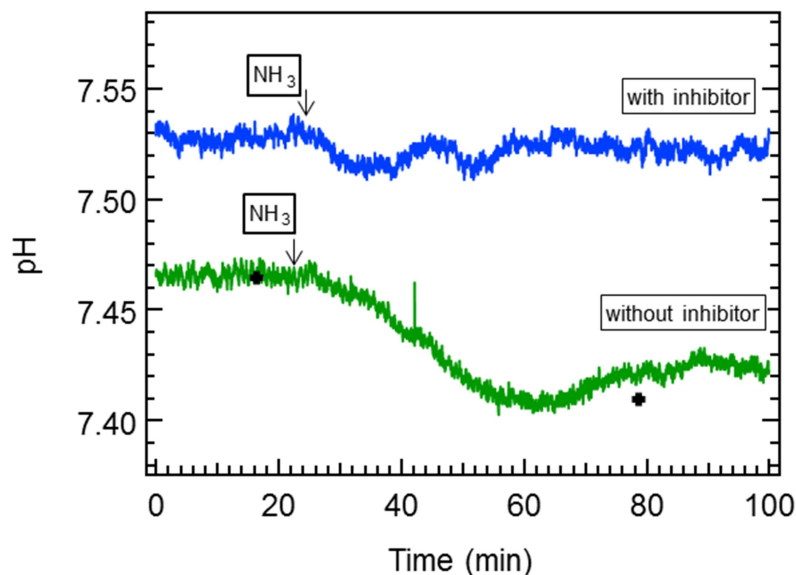

Figure 3. Changing pH inside the biofilm measured by the GFET sensor. A dose of NH$_3$ was added at $t = 21$ minutes. The blue curve was measured after the AMO enzyme was inhibited by ATU. The green curve was measured with no inhibitor. The black crosses correspond to measurements of the bulk pH.

We interpret the green curve as follows: at $t = 0$ (in the absence of NH$_3$) we assume that dissolved oxygen (DO) is present throughout the biofilm, as observed by Lauchnor et al.[22] After the addition of NH$_3$ there is lag time while NH$_3$ mixes/diffuses throughout the liquid. NH$_3$ consumption in the biofilm starts at $t \sim 25$ minutes as H$^+$ ions are generated and the local pH decreases. At $t = 60$ minutes, the supply of DO is diminished and the biofilm generates H$^+$ ions at a slower rate. As H$^+$ ions diffuse towards the bulk liquid and buffer diffuses into the biofilm, the

pH inside the biofilm begins to rise. At $t = 80$ minutes, nitrate levels have risen to 0.4 mM, which requires consumption of 0.6 mM of DO. The initial concentration of DO in our experiment was likely 0.3 mM (aqueous buffer in equilibrium with atmosphere). Since the medium was not stirred or aerated, slow mass transfer with the atmosphere explains the depletion of DO. The overall rate of NO_2^- formation is consistent with the observations of Lauchnor and Semprini for biofilms of *N. europaea* under conditions of oxygen limitation.[25]

Our interpretation of Fig. 3 assumes that the equilibration of the biofilm with the bulk fluid occurs on times scale of tens of minutes. We estimated the relevant equilibration times using methods described by Stewart[26] (see Supporting Information). The biofilm thickness was not measured therefore we assumed biofilm thickness of 1000 μm for calculation purposes. Lauchnor et al.[19,22] report biofilm thicknesses for *N. Europaea* of 200 to 400 μm when grown under conditions of higher shear. Based on a thickness of 1000 μm we estimate $t_{90} = 8$ minutes for NH_3. Since H^+ is distributed throughout the biofilm, gross estimates using this approach are not possible, however we would expect shorter diffusion times for H^+ due to its higher diffusivity in water. The equilibration times will be further lengthened by the boundary layer between the biofilm and the bulk fluid. We conclude that the time scales shown in Figure 3 are reasonable.

To check that the pH change shown in Fig. 3 is due to biofilm activity, we inhibited the biofilm's ability to consume NH_3. Allylthiourea (ATU) is known to completely inhibit nitrification of *N. europaea* biofilms by inhibiting the activity of the AMO enzyme.[22,27] The blue curve in Fig. 3 shows the response of the system after exposing the biofilm to ATU. The change in pH following the addition of NH_3 was not significantly different from the detector noise, confirming that the GFET is indeed sensitive to the nitrification activity of the biofilm.

Additional control tests measured the response of the GFET sensor before biofilm growth. The bare sensor shows no significant response or change in pH sensitivity in the presence of NH_3, ATU, NH_2OH, and NaN_3 (Figure S3). The bare sensor was also checked for response to changes in dissolved oxygen content and found to have no significant response (Figure S4).

Next, we studied the second step in NH_3 consumption, the utilization of NH_2OH via HAO activity,

$$NH_2OH + O_2 \xrightarrow{\text{HAO}} NO_2^- + H^+ + H_2O. \qquad (2)$$
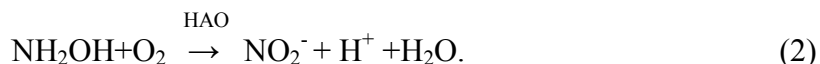
When *N. europaea* is supplied with NH_2OH, it produces one H^+ per oxidized NH_2OH molecule. Therefore, this sub-step in the NH_3 consumption pathway is also well suited to investigation using the GFET sensor.

The biofilm was inhibited by ATU (which inhibits AMO, but not HAO activity) and then dosed with 75 μmol of NH_2OH (resulting concentration ~ 1 mM). 6-7 minutes after introducing NH_2OH we observed a sharp downward spike in pH to 5.8, then a sharp increase (Fig. 4). Over the next 30 minutes, the pH inside the biofilm oscillates and finally stabilizes below the starting pH.
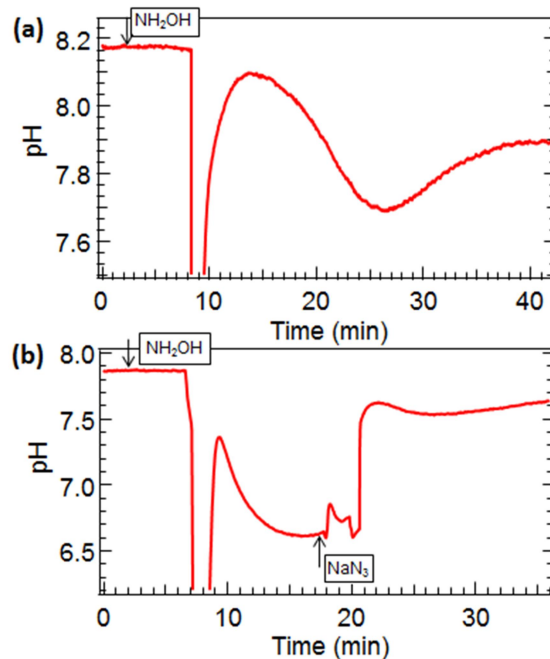
Figure 4. a) Response to NH_2OH. b) Response to NH_2OH followed by the biocide NaN_3.

The dramatic decrease in pH (Fig. 4) is strikingly different from that observed when adding a similar amount of NH_4^+ (Fig. 3). Figure S.X shows this test was repeated three times and the rapid decrease was very reproducible. Measurements of nitrite production, in response to NH_2OH addition, (see Figure S.4) showed about 70 % of the NH_2OH added was converted to nitrite in these tests, indicating rapid utilization. The potential for rapid utilization of NH_2OH by *N. europaea* in the acid pH range is supported by the kinetic studies of Frijlink et al.[28] They measured maximum utilization rates of NH_2OH at pH 5 of 53 nmol O_2/mg-min, compared to 169 nmol O_2/mg-min at pH 7. They also measured a half-substrate coefficient 198 µM at pH 5. Our bulk NH_2OH concentration of 1.0 mM is well above their measured K_s value, supporting the potential for high rates of NH_2OH utilization and H^+ formation even at a pH of 5. Oxygen mass balances, based on the nitrite formed, support the hypothesis that oxygen limitations likely

12

caused NH$_2$OH utilization to slow, which resulted in a rapid increase in pH. The formation of 0.8 mM of nitrite would require more oxygen than could have been initially present in the medium.

The rapid changes in pH detected by the GFET (Fig. 4) highlight the advantage of real-time sensing inside the biofilm. The dose of NH$_2$OH, above the K$_s$ value, and DO depletion likely caused rapid swings in local pH that are not observable in the bulk fluid. It appears that the first minutes of NH$_2$OH utilization likely resulted in low DO levels. Subsequent oscillations in pH suggest that the biofilm was responding to transient DO and NH$_2$OH concentrations. The ability to continuously monitor such temporal changes within a biofilm holds much promise.

The biofilm was dosed with NH$_2$OH two more times (11 hours later and 38 hours later, see Figure S.4). In both cases, the GFET recording of pH exhibited similar oscillatory behavior. The lag time between tests likely permitted DO to re-equilibrate with atmospheric oxygen, resulting in similar NH$_2$OH responses. Shortly after the final dose of NH$_2$OH, the biofilm was poisoned by the introduction of sodium azide (NaN$_3$) (Fig 4b). The pH inferred from the GFET biosensor indicates a sudden upward jump in pH 6 minutes after the addition of NaN$_3$. It should be noted that more liquid was introduced when NaN3 was added, which may have increased mass transfer into the biofilm, reducing the lag time between liquid injection and biofilm response.

We interpret the NaN$_3$ response as follows: in the period 1 to 6 minutes after the addition of NaN$_3$, the pH does not change dramatically, but the signal appears unstable. The biofilm microorganisms may still be alive, but increasingly vulnerable to perturbations due to a loss of resilience.[29] After 6 minutes, we interpret the jump in pH as a catastrophic collapse of the population as the local concentration of NaN$_3$ became lethal. The upward swing in pH is likely

caused by a sudden halt to H^+ production in the biofilm and a subsequent equilibration with the bulk fluid. While this interpretation is speculative, it suggests interesting directions for future research. It is particularly exciting to consider the possibility of detecting early warning signs of an impending population collapse. It also provides a potential *in-situ* method of monitoring processes used to control the growth of nitrifying biofilms in drinking water distribution systems.[30]

In conclusion, the GFET sensor was found to be a promising means of monitoring dynamic changes of pH inside a biofilm in response to changes in nitrification activity. The sensors are robust and long-lived, and low-cost production may be facilitated by graphene commercialization.[31] Future work will include the development of GFET sensor arrays, similar to charge-coupled device (CCD) image sensors, to perform spatially-resolved measurements of biofilm activity. The spatial resolution of such an array can easily be scaled to 3×3 μm^2.[17]

Supporting Information

Additional information as noted in the text. This material is available free of charge via the Internet at http://pubs.acs.org.

Corresponding Author

Ethan D. Minot: minote@science.oregonstate.edu

Author Contributions

The manuscript was written through contributions of all authors. All authors have given approval to the final version of the manuscript.

Funding Sources

(1)   Syron, E.; Casey, E. Critical Review Membrane-Aerated Biofilms for High Rate Biotreatment : Performance Appraisal , Engineering Principles , Scale-up , and Development Requirements. *Environ. Sci. Technol.* **2008**, *42*, 1833–1844.

(2)   Suidan, M. T. Performance of Deep Biofilm Reactors. *J. Environ. Eng.* **1986**, *112*, 78–93.

(3)   Denkhaus, E.; Meisen, S.; Telgheder, U.; Wingender, J. Chemical and physical methods for characterisation of biofilms. *Microchim. Acta* **2007**, *158*, 1–27.

(4)   Santegoeds, C. M.; Schramm, a; de Beer, D. Microsensors as a tool to determine chemical microgradients and bacterial activity in wastewater biofilms and flocs. *Biodegradation* **1998**, *9*, 159–167.

(5)   Liu, Y.; Dong, X.; Chen, P. Biological and chemical sensors based on graphene materials. *Chem. Soc. Rev.* **2012**, *41*, 2283–2307.

(6)   Li, J.; Wang, G.; Zhu, H.; Zhang, M.; Zheng, X.; Di, Z.; Liu, X.; Wang, X. Antibacterial activity of large-area monolayer graphene film manipulated by charge transfer. *Sci. Rep.* **2014**, *4*, 4359.

(7)   Bendali, A.; Hess, L. H.; Seifert, M.; Forster, V.; Stephan, A.-F.; Garrido, J. a; Picaud, S. Purified neurons can survive on peptide-free graphene layers. *Adv. Healthc. Mater.* **2013**, *2*, 929–933.

(8)   Stine, R.; Mulvaney, S. P.; Robinson, J. T.; Tamanaha, C. R.; Sheehan, P. E. Fabrication, optimization, and use of graphene field effect sensors. *Anal. Chem.* **2013**, *85*, 509–521.

(9)   Mohanty, N.; Berry, V. Resolution Biodevice and DNA Transistor : Interfacing Graphene Derivatives with Nanoscale and Microscale Biocomponents. **2008**.

(10)   Huang, Y.; Dong, X.; Liu, Y.; Li, L.-J.; Chen, P. Graphene-based biosensors for detection of bacteria and their metabolic activities. *J. Mater. Chem.* **2011**, *21*, 12358.

(11)   Mannoor, M. S.; Tao, H.; Clayton, J. D.; Sengupta, A.; Kaplan, D. L.; Naik, R. R.; Verma, N.; Omenetto, F. G.; McAlpine, M. C. Graphene-based wireless bacteria detection on tooth enamel. *Nat. Commun.* **2012**, *3*, 763.

(12)   Arp, D. J. et al. *The Nitrogen Cycle In Prokaryotic Nitrogen Fixation*; Triplett, E., Ed.; Horizon Scientific Press: Norfolk, U.K., 2000.

(13)   Prosser, J. I. Autotrophic Nitrification in Bacteria. *Adv. Microb. Physiol.* **1989**, 125–181.

(14)   Byers, J. D.; Lazarova, V.; Manem, I. *BiofilmsII*; Wiley: New York, 2000; pp. 159–206.

(15) EPA. U. S. Process Design Manual: Nitrogen Control. In; U.S. Environmental Protection Agency: Washington, D.C., 1993; p. 625/R – 93/010.

(16) Li, X.; Cai, W.; An, J.; Kim, S.; Nah, J.; Yang, D.; Piner, R.; Velamakanni, A.; Jung, I.; Tutuc, E.; et al. Large-area synthesis of high-quality and uniform graphene films on copper foils. *Science* **2009**, *324*, 1312–1314.

(17) Saltzgaber, G.; Wojcik, P.; Sharf, T.; Leyden, M. R.; Wardini, J. L.; Heist, C. A.; Adenuga, A. A.; Remcho, V. T.; Minot, E. D. Scalable graphene field-effect sensors for specific protein detection. *Nanotechnology* **2013**, *24*, 355502.

(18) Mailly-Giacchetti, B.; Hsu, A.; Wang, H.; Vinciguerra, V.; Pappalardo, F.; Occhipinti, L.; Guidetti, E.; Coffa, S.; Kong, J.; Palacios, T. PH sensing properties of graphene solution-gated field-effect transistors. *J. Appl. Phys.* **2013**, *114*.

(19) Lauchnor, E. G.; Radniecki, T. S.; Semprini, L. Inhibition and gene expression of Nitrosomonas europaea biofilms exposed to phenol and toluene. *Biotechnol. Bioeng.* **2011**, *108*, 750–757.

(20) Cui, Y.; Wei, Q.; Park, H.; Lieber, C. M. Nanowire nanosensors for highly sensitive and selective detection of biological and chemical species. *Science* **2001**, *293*, 1289–1292.

(21) Sharf, T.; Kevek, J. W.; Deborde, T.; Wardini, J. L.; Minot, E. D. Origins of charge noise in carbon nanotube field-effect transistor biosensors. *Nano Lett.* **2012**, *12*, 6380–6384.

(22) Lauchnor, E. G.; Semprini, L.; Wood, B. D. Kinetic parameter estimation in N. europaea biofilms using a 2-D reactive transport model. *Biotechnol. Bioeng. -in Press*.

(23) Suzuki, I.; Dular, U. Ammonia or Ammonium Ion Ammonia or Ammonium Ion as Substrate for Oxidation by Nitrosomonas europaea Cells and Extracts. *J. Bacteriol.* **1974**, *120*, 556–558.

(24) Lauchor, E. G. Inhibition, Gene expression and modeling of ammonia oxidation in biofilms of nitrosomonas europaea., Oregon State University, 2011.

(25) Lauchnor, E. G.; Semprini, L. Inhibition of phenol on the rates of ammonia oxidation by Nitrosomonas europaea grown under batch, continuous fed, and biofilm conditions. *Water Res.* **2013**, *47*, 4692–4700.

(26) Stewart, P. S. Guest Commentaries: Diffusion in Biofilms, Why is Diffusion an Important Process. **2003**, *185*, 1485–1491.

(27) Juliette, L. Y.; Hyman, M. R.; Arp, D. J. Mechanism-Based Inactivation of Ammonia Monooxygenase in Nitrosomonas europaea by Allylsulfide Mechanism-Based

Inactivation of Ammonia Monooxygenase in Nitrosomonas europaea by Allylsulfide. *Appl. Environ. Microbiol.* **1993**, *59*.

(28) Frijlink, M. .; Abee, T.; Laanbroek, H.; Beboer, W.; Konings, W. The bioenergetics of ammonia and hydroxylamine oxidation in Nitrosomonas europea at acid and alkaline pH. *Arch. Microbiol.* **1992**, *157*, 194–199.

(29) Dai, L.; Vorselen, D.; Korolev, K. S.; Gore, J. Generic indicators for loss of resilience before a tipping point leading to population collapse. *Science* **2012**, *336*, 1175–1177.

(30) Berry, D.; Xi, C.; Raskin, L. Microbial ecology of drinking water distribution systems. *Curr. Opin. Biotechnol.* **2006**, *17*, 297–302.

(31) Zurutuza, A.; Marinelli, C. Challenges and opportunities in graphene commercialization. *Nat. Nanotechnol.* **2014**, *9*, 730–734.